2.0 mmol), and a mixture of deionized water (degassed, 3 ml) and methanol (12 ml) were added to a 50 ml round-bottom flask with a stir bar. The macromonomer OEGMA (8 g, 16.7 mmol) was added and the dark red solution was bubbled with nitrogen for 30 min. The mixture was transferred by a syringe to the funnel and purged with nitrogen for 5 min. Polymerization was initiated by adding the mixture into the flask and was continued for a specified time (10–720 min) under nitrogen purge. The samples were pulled out of the solution to stop the polymerization, rinsed with methanol, and dried under flowing nitrogen.

Ellipsometry: Film thickness was measured on a M-88 spectroscopic ellipsometer (J. A. Woollam Co., Inc) at angles of 65°, 70°, and 75° and wavelengths from 400 nm to 800 nm. Ellipsometric data were fitted for thickness of SAMs and poly(OEGMA) film with fixed (A_n, B_n) values of (1.45, 0.01), and (1.46, 0.01), respectively using a Cauchy layer model [9]. The ellipsometric thickness for each sample was independently measured at three different locations and is reported as the average ± standard deviation (sd).

Received: August 11, 2003
Final version: October 21, 2003

[1] J. M. Harris, in *Poly(Ethylene Glycol) Chemistry: Biotechnical and Biomedical Applications* (Ed: J. M. Harris), Plenum Press, New York **1992**, pp. 1–14.
[2] M. Mrksich, L. E. Dike, J. Tien, D. E. Ingber, G. M. Whitesides, *Exp. Cell Res.* **1997**, *235*, 305.
[3] M. Mrksich, G. M. Whitesides, in *American Chemical Society Symposium Series on Chemistry and Biological Applications of Polyethylene Glycol 680* (Eds: J. M. Harris, S. Zalipsky), ACS, Washington, DC **1997**, pp. 361–373.
[4] B. Zhao, W. J. Brittain, *Prog. Polym. Sci.* **2000**, *25*, 677.
[5] J. H. Lee, J. D. Andrade, in *Polymer Surface Dynamics* (Ed: J. D. Andrade), Plenum Press, New York **1988**, pp. 119–136.
[6] J. H. Lee, J. Kopecek, J. D. Andrade, *J. Biomed. Mater. Res.* **1989**, *23*, 351.
[7] D. L. Elbert, J. A. Hubbell, *J. Biomed. Mater. Res.* **1998**, *42*, 55.
[8] V. A. Liu, W. E. Jascromb, S. N. Bhatia, *J. Biomed. Mater. Res.* **2002**, *60*, 126.
[9] K. L. Prime, G. M. Whitesides, *J. Am. Chem. Soc.* **1993**, *115*, 10 714.
[10] N. Xia, Y. H. Hu, D. W. Grainger, D. G. Castner, *Langmuir* **2002**, *8*, 3255.
[11] J. P. Bearinger, S. Terrettaz, R. Michel, N. Tirelli, H. Vogel, M. Textor, J. A. Hubbell, *Nat. Mater.* **2003**, *2*, 259.
[12] C. Nojiri, T. Okano, H. A. Jacobs, K. D. Park, S. F. Mohammad, D. B. Olsen, S. W. Kim, *J. Biomed. Mater. Res.* **1990**, *24*, 1151.
[13] Y. H. Sun, W. R. Gombotz, A. S. Hoffman, *J. Bioact. Compat. Polym.* **1986**, *1*, 316.
[14] E. W. Merrill, K. A. Wright, A. Sagar, R. W. Pekala, K. A. Dennison, S.-W. Tay, C. Sung, E. Chaikof, P. Rempp, P. Lutz, A. D. Callow, R. Connolly, K. Ramberg, S. Verdon, in *Polymers In Medicine: Biomedical & Pharmaceutical Applications* (Eds: R. M. Ottenbrite, E. Chiellini), Technomic, Lancaster, PA **1992**, pp. 39–56.
[15] P. Ghosh, M. L. Amirpour, W. M. Lackowski, M. V. Pishko, R. M. Crooks, *Angew. Chem. Int. Ed.* **1999**, *38*, 1592.
[16] G. P. López, B. D. Ratner, C. D. Tidwell, C. L. Haycox, R. J. Rapoza, T. A. Horbett, *J. Biomed. Mater. Res.* **1992**, *26*, 415.
[17] Y. T. Kim, A. J. Bard, *Langmuir* **1992**, *8*, 1096.
[18] C. Schönenberger, J. A. M. Sondag-Huethorst, J. Jorritsma, L. G. Fokkink, *Langmuir* **1994**, *10*, 611.
[19] X.-M. Zhao, J. L. Wilbur, G. M. Whitesides, *Langmuir* **1996**, *12*, 3257.
[20] M. J. Tarlov, J. G. Newman, *Langmuir* **1992**, *8*, 1398.
[21] M. H. Schoenfisch, J. E. Pemberton, *J. Am. Chem. Soc.* **1998**, *120*, 4502.
[22] D. M. Jones, A. A. Brown, W. T. S. Huck, *Langmuir* **2002**, *18*, 1265.
[23] R. G. Nuzzo, D. L. Allara, *J. Am. Chem. Soc.* **1990**, *105*, 4481.
[24] K. Matyjaszewski, J. H. Xia, *Chem. Rev.* **2001**, *101*, 2921.
[25] K. Matyjaszewski, P. J. Miller, N. Shukla, B. Immaraporn, A. Gelman, B. B. Luokala, T. M. Siclovan, G. Kickelbick, T. Vallant, H. Hoffmann, T. Pakula, *Macromolecules* **1999**, *32*, 8716.
[26] *BIAtechnology Handbook* (Pharmacia Biosensor AB, Sweden), **1994**.
[27] a) R. L. C. Wang, H. T. Kreuzer, M. Grunze, *J. Phys. Chem. B* **1997**, *101*, 9767. b) A. J. Pertsin, T. Hayashi, M. Grunze, *J. Phys. Chem. B* **2002**, *106*, 12 274. c) D. Schwendel, T. Hayashi, R. Dahint, A. Pertsin, M. Grunze, R. Steitz, F. Schreiber, *Langmuir* **2003**, *19*, 2284. d) S. Herrwerth, W. Eck, S. Reinhardt, M. Grunze, *J. Am. Chem. Soc.* **2003**, *125*, 9359.
[28] a) R. R. Shah, D. Merreceyes, M. Husemann, I. Rees, N. L. Abbott, C. J. Hawker, J. L. Hedrick, *Macromolecules* **2000**, *33*, 596. b) D. M. Jones, W. T. S. Huck, *Adv. Mater.* **2001**, *13*, 1256. c) J. Hyun, A. Chilkoti, *Macromolecules* **2001**, *34*, 5644. d) M. R. Tomlinson, T. Wu, K. Efimenko, Genzer, *J. Polym. Prepr. (Am. Chem. Soc., Div. Polym. Chem.)* **2003**, *44*, 468.
[29] A. Kumar, G. M. Whitesides, *Appl. Phys. Lett.* **1993**, *63*, 2002.
[30] a) R. D. Piner, J. Zhu, F. Xu, S. Hong, C. A. Mirkin, *Science* **1999**, *283*, 661. b) J. Hyun, S. J. Ahn, W. K. Lee, A. Chilkoti, S. Zauscher, *Nano Lett.* **2002**, *2*, 1203.
[31] U. Schmelmer, R. Jordan, W. Geyer, W. Eck, A. Gölzhäuser, M. Grunze, A. Ulman, *Angew. Chem. Int. Ed.* **2003**, *42*, 559.
[32] T. A. Horbett, *Colloid Surf., B* **1994**, *2*, 225.
[33] NIH 3T3 fibroblast cells: a continuous cell line of highly contact-inhibited cells was established from NIH Swiss mouse embryo cultures in the same manner as the original random-bred 3T3 (ATCC CCL-92) and the inbred BALB/c 3T3 (ATCC CCL-163). The established NIH/3T3 line was subjected to more than 5 serial cycles of subcloning in order to develop a subclone with morphologic characteristics best suited for transformation assays. a) J. L. Jainchill, S. A. Aaronson, G. J. Todaro, *J. Virol.* **1969**, *4*, 549. b) P. Andersson, M. P. Goldfarb, R. A. Weinberg, *Cell* **1979**, *16*, 63. c) N. G. Copeland, G. M. Cooper, *Cell* **1979**, *16*, 347.
[34] a) D. J. Irvine, L. G. Griffith, A. M. Mayes, *Biomacromolecules* **2001**, *2*, 85. b) X. Jiang, P. T. Hammond, *Polym. Mater. Sci. Eng.* **2001**, *84*, 172. c) J. Hyun, H. Ma, P. Banerjee, J. Cole, K. Gonsalves, A. Chilkoti, *Langmuir* **2002**, *18*, 2975.
[34] J. Hyun, H. Ma, Z. Zhang, T. P. Beebe, Jr., A. Chilkoti, *Adv. Mater.* **2003**, *15*, 576.

Engineered Planar Defects Embedded in Opals**

By *Elisa Palacios-Lidón*, *Juan F. Galisteo-López*, *Beatriz H. Juárez*, and *Cefe López**

Photonic crystals (PCs) are materials exhibiting a periodic modulation in the refractive index that has the effect of opening forbidden energy ranges, known as gaps.[1,2] Consequently,

[*] Dr. C. López, E. Palacios-Lidón, J. F. Galisteo López, B. H. Juárez
Instituto de Ciencia de Materiales de Madrid (CSIC)
Cantoblanco, E-28049 Madrid (Spain)
E-mail: cefe@icmm.csic.es

[**] This work is partially financed by the Comunidad Autónoma de Madrid though 07T/0048/2003 and Spanish MCyT through MAT 2003-01 237 projects. We gratefully acknowledge Florencio García-Santamaría for helpful discussions.

DOI: 10.1002/adma.200306172

ADVANCED MATERIALS

photons of energy within this gap cannot propagate through the crystal. The use of artificial opals as photonic crystals has been stimulated because they are a cheap and easy alternative to the more sophisticated PCs fabricated by lithography or holographic lithography.[3] The methods for opal synthesis are based on the natural tendency of microspherical colloids (e.g., silica, polystyrene (PS), poly(methyl methacrylate) (PMMA)) to self-assemble in an ordered face-centered-cubic (fcc) structure. One of the most commonly used is the vertical deposition method[4] that produces samples exhibiting large ordered areas (on the order of square centimeters). Although these structures exhibit interesting optical properties by themselves,[5] they can be used as a starting point for the preparation of more sophisticated systems, allowing the modification of their optical properties almost at will. For example, by void infiltration with a high-refractive-index material, PCs with full photonic bandgaps (PBGs) in the near-infrared (NIR) and visible range can be produced.[6,7] Recent work has shown that "band engineering" is possible by infiltration of different materials in a multilayered way.[8,9] Silica and PS spheres containing a metallic or magnetic core can be synthesized, allowing coupling of the metallic and/or magnetic properties with the photonic ones.[10,11] Using patterned surfaces as substrates, the fabrication of prisms[12] and microfibers[13] made of PCs is possible. Another methodology is the introduction of controlled defects in colloidal crystals by use of two-photon polymerization[14] or laser microannealing.[15] By combining spheres of two different sizes, ordered superlattices[16] or structures containing planar defects[17] have recently been obtained.

In this paper, we present an innovative method that allows the fabrication of opal slab heterostructures incorporating engineered planar defects. The method is based on a multi-step process that combines the ability to grow high-quality, controlled-thickness opals by convective colloidal self-assembly[4] and oxide infiltration by chemical vapor deposition (CVD) (Fig. 1). The method allows precise control over the parameters that determine the optical properties of these systems, permitting their tuning. Experimental evidence of the feasibility of the method, as well as the optical properties of the fabricated structures, is presented. As will be shown, this method is of relevance in the field of PCs since it constitutes a cheap and straightforward way of fabricating devices based on opals.

Silica (SiO_2) was chosen as the most suitable material for infiltration because it is one of the most important materials used in optical communications technology. Additionally, it has been studied for years and its physical and chemical properties are well characterized.[18] It can serve as a host for rare earth luminescent ions.[19] Furthermore, it is transparent in the visible and NIR range, and inert at ambient conditions and the high temperatures needed for the polymer matrix calcination (450 °C) involved in the presented method. Until now, silica infiltration of PS or PMMA opals has been performed via sol–gel,[20,21] which presents two problematic issues: infiltration usually yields inhomogeneous samples, and in the gel step the material usually expands causing cracks that limit the domain size of the opal. We have used an alternative method to infiltrate PS opals with SiO_2 (SiO_2/PS opal), consisting of a CVD technique working at room temperature and atmospheric pressure, initially developed by Ozin and co-workers, to increase the mechanical stability of SiO_2 opals.[22] By controlling some CVD parameters, such as time, gas flow rate, and number of cycles, high precision can be achieved in the filling fraction. Figure 2a shows an inverse silica opal resulting from the removal of the polymer matrix by calcination. The existence of large domains is clearly evidenced and the only disorder

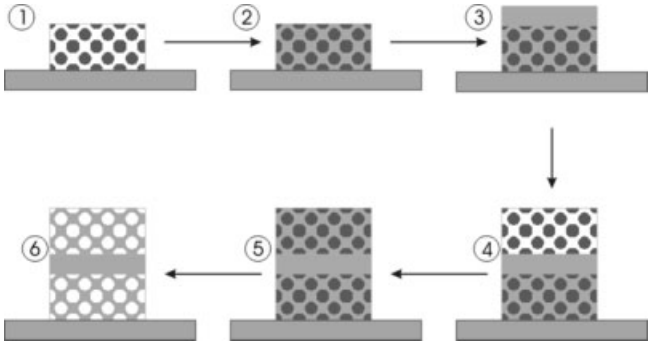

Figure 1. Diagram of the method: Planar defects in the studied opals were created using a six-step process: 1) Growth of a thin film PS opal by convective assembly; 2) CVD Infiltration of the PS matrix; 3) growth of a silica film of desired thickness by CVD; 4) growth of a new opal crystal as in step 1; 5) full infiltration of the new (bare) opal; 6) removal of the polymer matrix by calcination.

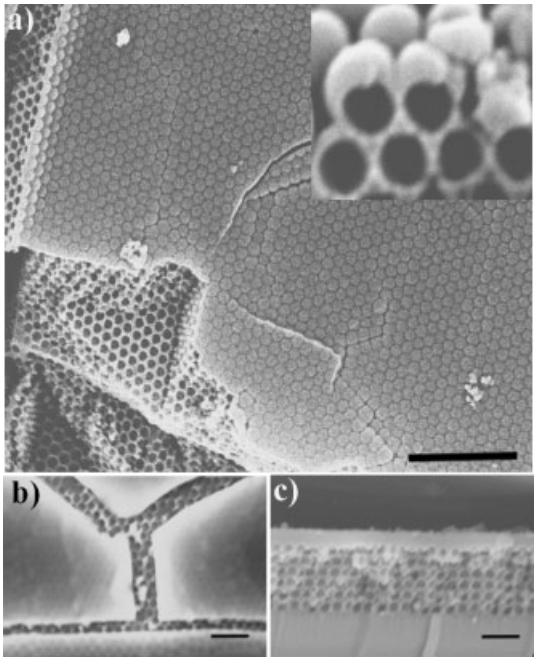

Figure 2. a) Silica inverse opal obtained by CVD after removing the PS matrix. The SEM photograph shows the homogeneity of the sample (scale bar 5 μm). Inset: detail of the opal surface. It can be clearly seen that it is made of hollow silica shells of uniform thickness. b) Silica film grown on top of a silica inverse opal. The sample has been inverted to enhance SEM contrast. c) Cleaved edge of the same sample. A uniform film of 280 nm is clearly seen on the top of the sample. Scale bars in (b,c) are 400 nm.

present in the sample originates from the template itself. Silica has grown covering the PS spheres homogeneously across the whole sample both in terms of depth (more than thirty layers) and width (on the order of square centimeters). The silica film grows in a layered way, faithfully replicating the sphere topography by forming a film of uniform thickness, as can be seen in the inset of Figure 2a, where the corrugation of the inverse opal surface is clearly appreciable.

The same CVD method is used to grow silica thin films on top of fully infiltrated opals. The method is first tested on clean substrates, finding that very flat and homogeneous thin films are obtained. In order to determine the thickness dependence of the silica film on growth parameters, different films were grown on different substrates (glass, silicon, mica) by changing the CVD working conditions. Profilometry measurements, scanning electron microscopy (SEM), and reflectance spectroscopy (not shown) were carried out to determine the growth rate. It was found that, after the formation of a thin coating (~10 nm) in the first stage, which is highly dependent on the hydrophilic character of the substrate, the subsequent growth of thicker films is substrate independent, and several micrometers thick silica films with nanometer uncertainty can be obtained. This fact allows the preparation of a thin silica film of controlled thickness on top of a previously infiltrated SiO_2/PS opal. Figure 2b shows a SEM photograph of a 280 nm silica film covering an inverse silica opal. The sample has been inverted by calcination to obtain more contrast in the SEM images. Through a crack produced during the polymer removal process, the inverse opal can be seen under the flat film. By inspection of a cleaved edge (Fig. 2c) the uniformity of the film thickness can be observed.

Deposition of a new thin-film opal of different PS sphere size on top of a SiO_2/PS composite has been carried out. This additional growth leads to the formation of an opal slab heterostructure made of two PC stacks; the first located at the bottom, corresponding to the initial SiO_2/PS composite opal, and a new PS bare opal grown on top. After infiltration of the bare stack and further removal of the PS spheres, an inverse silica heterostructure is achieved. The final heterostructure, along with reflectance measurements obtained after every step, is shown in Figure 3. In this system, the difference in sphere sizes is great enough that the diffraction peaks associated with each opal do not overlap. As was previously reported,[16] in this situation the optical response of this heterostructure system is the sum of the individual systems. It is important to notice that after the second opal has been grown, the Bragg peak associated with the old one has slightly shifted in wavelength. This can be accounted for by the change in the surrounding medium.[5] The oscillations shown in the spectra due to the finite thickness of the sample reveal a high quality, also evidenced through SEM inspection (Fig. 3d). It can be seen that a good interface between the two opals is obtained due to the thin silica layer, which planarizes the surface before regrowth.

By combining the two previously referred procedures, it is possible to engineer designed planar defects inside a PC just

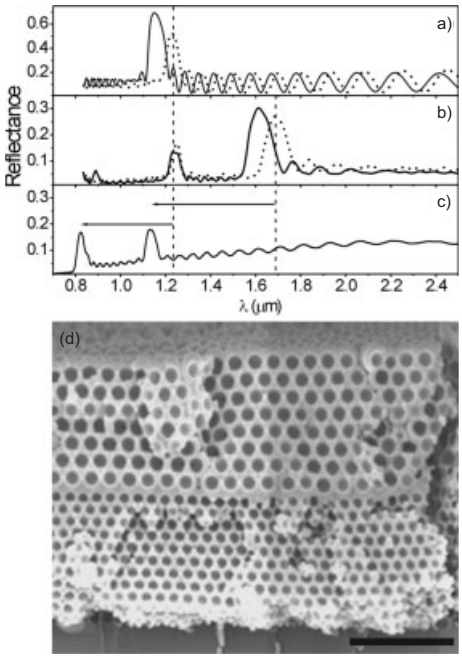

Figure 3. a) Experimental reflectance spectra of an opal slab made of 500 nm PS spheres before (solid line) and after complete infiltration with SiO_2 (dotted line). The Bragg peak is shifted to higher wavelengths (lower energies) as the mean refractive index increases. b) Reflectance spectra after a second opal made of 700 nm spheres is grown (solid line) on the top of the composite. Bragg peaks associated with both structures can be observed, separated in wavelength due to the difference in sphere size. After a new infiltration with silica (dotted line), a spectral shift appears only for the Bragg peak associated with the second (top) opal (no further infiltration takes place for the buried one). c) When this structure is calcinated, the spectrum shows two peaks corresponding to the two individual silica inverse opals. d) SEM photograph of the final structure (scale bar 3 μm).

by creating a heterostructure made of two opal slabs of the same sphere size separated by a flat and uniform silica sheet of the desired thickness. It is well known that breaking the periodicity in a photonic crystal by the introduction of a defect produces the appearance of localized states for photons within the gap. The spectral position of the state depends both on the nature (i.e., refractive index) and thickness of the defect, as well as the characteristics of the surrounding PC. The first experimental evidence was produced by Yablonovich et al.,[23] who introduced point defects in a PC working in the microwave range. Watson and co-workers[24] introduced point defects in colloidal suspensions working in the visible range. Recently, some groups have proved the existence of localized states in silica opals by changing the sphere size of one of the planes.[17] We chose to break the lattice periodicity by inserting a homogeneous sheet of material. Figure 4 shows the reflectance and transmission spectra of one such system, with a planar defect made of a 460 nm silica film between two SiO_2/PS opals of 311 nm sphere size. A sharp resonance in the Bragg peak associated with the defect state is apparent in both the transmittance (T) and reflectance (R) at the same spectral position. Comparing this peak with the defect-free

ADVANCED MATERIALS

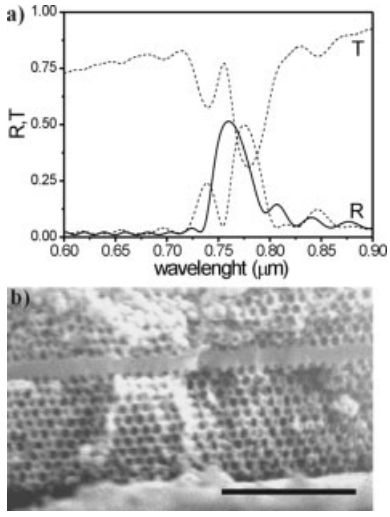

Figure 4. a) Experimental reflectance and transmittance (dashed lines) of a PC with a planar defect inserted. The heterostructure comprises two SiO_2/PS opals separated by a 460 nm silica film. The reflectance spectrum of the host opal has been included (solid line). b) SEM photograph of a cleaved edge of the structure that has been inverted for clarity. A uniform silica film is clearly seen between the two opal slabs.

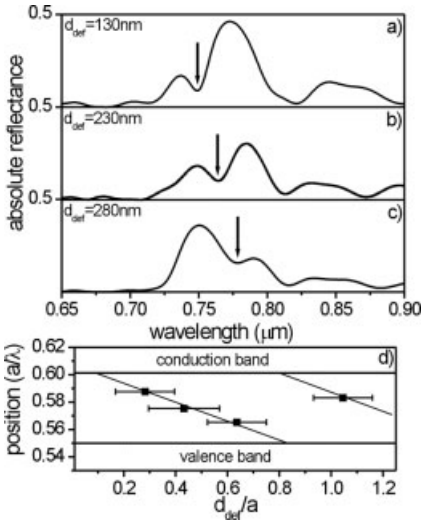

Figure 5. Reflectance spectra of engineered defects in 311 nm SiO_2/PS opals. Silica film planar defects of a) 130 nm, b) 230 nm, and c) 280 nm are embedded in the photonic crystal. Depending on the defect thickness the dip position shifts through the gap, starting at low wavelengths (high energies). d) Spectral position as a function of defect thickness. The straight lines are guides to the eye.

opal, a clear broadening is found. Similar behavior was previously presented in the literature.[24] In the SEM photograph (Fig. 4b), the silica film is clearly seen. The fact that the growth takes place on a glass substrate prevents proper cleavage and spoils the fracture facet.

In order to study the spectral position dependence of the defect state on film thickness, samples with fifteen layers of 311 nm PS spheres on both the top and bottom opal slabs were prepared; the silica film thickness inserted between them was varied. It is important that the two opal slabs confining the silica sheet have the same number of layers in order to match the spectral position and width of their respective Bragg peaks,[5] which will contribute to improve its performance as a cavity. The thickness of the SiO_2 film was checked using SEM images. The reflectance spectra (Fig. 5) show that the expected resonance appears at the conduction band edge and moves through the photonic gap (Bragg peak) to lower energy as the defect thickness increases, until it reaches the valence band when the silica film thickness is of the order of the sphere size. In this system the planar defect gives rise to an acceptor mode.[25,26] Such behavior was theoretically predicted[26] for a system similar to that used in this study, assuming two photonic crystal slabs separated by a known variable distance. If the film thickness is larger than the sphere size the resonance re-enters at the high-energy side of the gap and the process starts again. In Figure 5d the spectral position of a $1.045\,a$ (where a is the lattice parameter) defect state has been included. Its energy coincides with that expected for a $0.339\,a$ defect. Without deeper modal analysis, it may be seen from this result that the resonance energy is a phenomenon that depends on the ratio of the slab thickness to the sphere size, and indirectly, to the lattice parameter.

To study the dependence of the resonance spectral position on the PC lattice parameter, two samples with different sphere size containing a 460 nm silica film were prepared. Their respective reflectance spectra (Fig. 6) show that the position of the localized state relative to the centre of the Bragg peak is different. This can be understood by expressing the re-

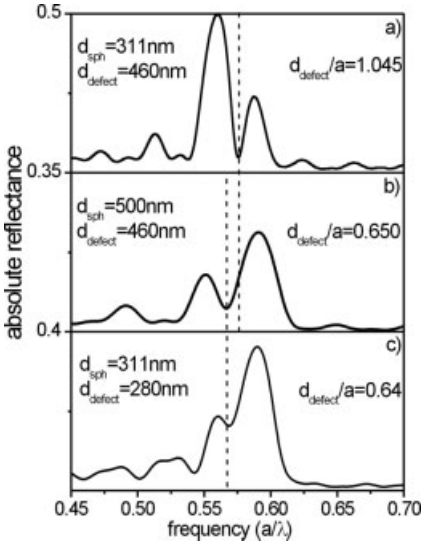

Figure 6. Reflectance spectra of a 460 nm engineered defect, embedded in a) 311 nm and b) 500 nm sized sphere SiO_2/PS opals. While for the 311 nm sphere opal the resonance appears close to the conduction band edge, in the 500 nm sphere opal it is situated near the valence band. c) Reflectance spectra of a 280 nm silica defect embedded in a 311 nm sized sphere SiO_2/PS opals. The scalability of the system is clearly seen by realizing that the state position depends only on the defect thickness/lattice parameter ratio (d/a).

sults in units of the lattice parameter and keeping in mind that the underlying theory is scalable. With that understanding, two samples with different spheres size and different silica film thickness but the same defect thickness/lattice parameter ratio are compared, finding that the resonance position coincides (Fig. 6).

The structures studied, although lacking a full PBG, could nevertheless be used for conventional light guiding by total internal reflection. When operating at energies below the low-frequency edge of the pseudo-gap, the inverse opals confining the cavity behave as a medium with an effective refractive index smaller than that of pure silica, which constitutes the guide, and thus allows total internal reflection. By changing the material constituting the inverse opals that confine the planar defect for materials with larger refractive indices (e.g., silicon or germanium), which would open a full PBG, the quality factor of the cavity could be enhanced, allowing for a better confinement of the photons at the defect. This would improve the performance of the structures both as a cavity for laser action and as a planar wave guide, in which light guiding would take place by Bragg diffraction.

In summary, we have presented an easy-to-implement method that allows the fabrication of a vast range of structures based on artificial opals, such as silica inverse opals and opal slab heterostructures, presenting a very versatile optical response. Through the combination of spheres of different sizes and chemical nature (silica or PMMA), and by the selection of different materials with a higher refractive index more complex structures with very interesting optical properties can be built up. We have produced engineered planar defects inside a PC that can act as photonic microcavities. We have demonstrated the possibility of tuning the localized state spectral position introduced by the defect changing its thickness as well as the scalability of the problem.

Experimental

PS spheres have been synthesized by a surfactant-free emulsion method [27]. Thin film opals were grown in a glass vial by the vertical deposition method [4] using a suspension of 0.3 wt.-% of PS spheres in water. A clean glass microscope slide, used as the substrate, was placed vertically in the vial and left in the oven at 45 °C for 24 h.

Silica infiltration was performed following the CVD method proposed in the literature [22]. The sample was placed in a home-made glass reactor working at room temperature and atmospheric pressure. Silicon tetrachloride ($SiCl_4$) and doubly distilled water (DDW) were used as precursors. They were separately bubbled, starting with the DDW, by a N_2 flow that carried the vapor phases to the reactor containing the sample. The CVD process simply consists of the hydrolysis of $SiCl_4$ taking place on the surface [28] of the hydrophilic spheres that have previously been wetted. SiO_2 coating can easily be controlled by the N_2 flow rate and the exposure time used.

All reflectance and transmission spectra were acquired at incidence normal to the (111) direction from regions about 400 μm^2 in size in a commercial Fourier transform infrared (FTIR) spectrophotometer (Bruker IFS 66 with IRScope II). The optical spectra shown in this study are raw spectra without any further data processing. The quality of the achieved structure in every step is checked through optical measurements and SEM inspection.

Received: September 15, 2003
Published online: January 30, 2004

[1] E. Yablonovitch, *Phys. Rev. Lett.* **1987**, *58*, 2085.
[2] S. John, *Phys. Rev. Lett.* **1987**, *58*, 2486.
[3] C. López, *Adv. Mater.* **2003**, *15*, 1679.
[4] P. Jiang, J. F. Bertone, K. S. Hwang, V. L. Colvin, *Chem. Mater.* **1999**, *11*, 2132.
[5] J. F. Galisteo-López, E. Palacios-Lidón, E. Castillo-Martinez, C. López, *Phys. Rev. B* **2003**, *68*, 115 109.
[6] A. Blanco, E. Chomski, S. Grabtchak, M. Ibisate, S. John, S. W. Leonard, C. López, F. Meseguer, H. Míguez, J. P. Mondia, G. A. Ozin, O. Toader, H. M. van Driel, *Nature* **2000**, *405*, 437.
[7] B. H. Juarez, M. Ibisate, J. M. Palacios, C. López, *Adv. Mater.* **2003**, *15*, 319.
[8] F. Garcia-Santamaria, M. Ibisate, I. Rodriguez, F. Meseguer, C. López, *Adv. Mater.* **2003**, *15*, 788.
[9] H. Miguez, S. M. Yang, N. Tetreault, V. Kitaev, G. A. Ozin, *Adv. Mater.* **2003**, *15*, 597.
[10] F. Garcia-Santamaria, V. Salgueirino-Maceira, C. López, L. M. Liz-Marzan, *Langmuir* **2002**, *18*, 4519.
[11] X. L. Xu, G. Friedman, K. D. Humfeld, S. A. Majetich, S. A. Asher, *Chem. Mater.* **2002**, *14*, 1249.
[12] Y. D. Yin, Y. N. Xia, *Adv. Mater.* **2002**, *14*, 605.
[13] H. Miguez, S. M. Yang, N. Tetreault, G. A. Ozin, *Adv. Mater.* **2002**, *14*, 1805.
[14] W. M. Lee, S. A. Pruzinsky, P. V. Braun, *Adv. Mater.* **2002**, *14*, 271.
[15] N. Tétreault, H. Míguez, S. M. Yang, V. Kitaev, G. A. Ozin, *Adv. Mater.* **2003**, *15*, 1167.
[16] P. Jiang, G. N. Ostojic, R. Narat, D. M. Mittleman, V. L. Colvin, *Adv. Mater.* **2001**, *13*, 389.
[17] K. Wostyn, Y. Zhao, G. de Schaetzen, L. Hellemans, N. Matsuda, K. Clays, A. Persoons, *Langmuir* **2003**, *19*, 4465.
[18] *CRC Handbook of Chemistry and Physics* (Ed: D. R. Lide), CRC Press, Boca Raton, FL **2001**.
[19] A. Polman, *J. Appl. Phys.* **1997**, *82*, 1.
[20] O. D. Velev, T. A. Jede, R. F. Lobo, A. M. Lenhoff, *Nature* **1997**, *389*, 447.
[21] B. T. Holland, C. F. Blanford, T. Do, A. Stein, *Chem. Mater.* **1999**, *11*, 795.
[22] H. Miguez, N. Tetreault, B. Hatton, S. M. Yang, D. Perovic, G. A. Ozin, *Chem. Commun.* **2002**, *22*, 2736.
[23] E. Yablonovitch, T. J. Gmitter, R. D. Meade, A. M. Rappe, K. D. Brommer, J. D. Joannopoulos, *Phys. Rev. Lett.* **1991**, *67*, 3380.
[24] R. D. Pradhan, I. I. Tarhanm, G. H. Watson, *Phys. Rev. B* **1996**, *54*, 721.
[25] W. Suh, M. F. Yanik, O. Solgaard, S. Fan, *Appl. Phys. Lett.* **2003**, *82*, 1999.
[26] V. Karathanost, A. Modinos, N. Stefanous, *J. Phys. Condens. Matter* **1994**, *6*, 6257.
[27] J. W. Goodwin, J. Hearn, C. C. Ho, R. H. Ottewill, *Colloid Polym. Sci.* **1974**, *252*, 464.
[28] C. J. Brinker, G. W. Scherer, *Sol-Gel Science*, Academic Press, London **1990**.

